SAG: Stars and Galaxies **Vol. 8**, id. 4, 2025 December 28

Revisiting the near-infrared color of Karin family asteroids

Shigeru TAKAHASHI[1], Fumi YOSHIDA[2,3], Hikaru KUBOTA[4], Hideo SAGAWA[5,6], and Takahiro IINO[6]
[1]*Nishi-Harima Astronomical Observatory, Center for Astronomy, University of Hyogo,407–2 Nishigaichi, Sayo-cho, Hyogo 679–5313, Japan*
[2]*University of Occupational and Environmental Health, Japan, 1-1 Iseigaoka, Yahata, Kitakyusyu, Fukuoka 807-8555, Japan*
[3]*Planetary Exploration Research Center, Chiba Institute of Technology, 2-17-1 Tsudanuma, Narashino, Chiba 275-0016, Japan*
[4]*Division of Science, Graduate School, Kyoto Sangyo University, Kamigamo Motoyama, Kita, Kyoto 603-8555, Japan*
[5]*Faculty of Science, Kyoto Sangyo University, Kamigamo Motoyama, Kita-ku, Kyoto 603-8555, Japan*
[6]*Information Technology Center, The University of Tokyo, 2-11-16 Yayoi, Bunkyo-ku, Tokyo 113-8658, Japan*
shigeru@nhao.jp

(Received 2025 October 28; accepted 2025 December 19)

Abstract

We conducted a near-infrared spectrophotometric study of the Karin family asteroids; (832) Karin, (13765) Nansmith, (47640) 2000 CA30, (69880) 1998 SQ81, and a non-Karin family member (4507) Petercollins (1990 FV), using the ground-based near-infrared images taken at the UKIRT on Mauna Kea. Several previous observations have reported that (832) Karin has two distinct surface types: a red surface and a non-red surface. We detected the non-red surface. By combining our data with the previous observations, we attempted to locate the position of the red surface but could not find a clear solution that satisfies all the observational results. For the other asteroids in the Karin family, except for (47640) 2000 CA30, their colors were nearly identical to that of (832) Karin. On the other hand, (4507) Petercollins, which has been suggested to be an interloper in the Karin family, exhibited a redder surface than the other Karin family asteroids. This is consistent with the study that (4507) Petercollins is not a member of the Karin family.

Key words: Asteroid — Near-Infrared — Spectrophotometry — (832) Karin

1. Introduction

"Collision" is one of the key processes for understanding the formation and evolution of the Solar System. The physical properties of asteroids may retain traces of past collisions between celestial bodies, and therefore theoretical and observational studies of various asteroid properties such as surface color, shape, and rotational velocity have been used to infer the characteristics of frequent collisions in the Solar System history (e.g., Zappalà et al. 1984; Davis et al. 1989).

In 2002, using numerical integration techniques that trace the current orbital motion of asteroids back in time, a young subgroup within the long-known Koronis family was discovered (Nesvorný et al. 2002). This subgroup was named the Karin family, after its largest member, (832) Karin. According to the numerical integration work by Nesvorný et al. (2002), the Karin family was formed in a collisional breakup event only 5.8 million years ago, and 39 Karin family asteroids have since been identified.

Since the report from Nesvorný et al. (2002), several observational studies have been conducted on (832) Karin and the Karin family of asteroids (Yoshida et al. 2004; Sasaki et al. 2004; Vernazza et al. 2006; Chapman et al. 2007; Vernazza et al. 2007; Ito & Yoshida 2007; Harris et al. 2009; Yoshida et al. 2016).

Among them, Sasaki et al. (2004) discovered spectral variations on the surface of (832) Karin through near-infrared observations made with the Subaru Telescope on September 14, 2003. They obtained three sets of spectra and found that the first set was considerably redder (referred to as "red") than the other two sets (referred to as "non-red"). They suggested that this spectral difference might be due to varying degrees of space weathering on (832) Karin's surface. In other words, Sasaki et al. (2004) proposed that the "red" area could be more space-weathered than the "non-red" areas. Observations by Yoshida et al. (2004) in visible bands also reported variations in the surface colors of (832) Karin. These findings led to further research aimed at confirming the surface heterogeneity of (832) Karin.

In 2004, Ito & Yoshida (2007) conducted color observations at visible wavelengths over one rotation phase of (832) Karin and observed only "non-red" surfaces. They attributed the homogeneous results in 2004 to geometric differences between the 2003 and 2004 observations. In 2006, near-infrared spectroscopic observations (Chapman et al. 2007) and visible/near-infrared spectroscopic observations (Vernazza et al. 2007), which covered one rotation phase, were conducted. However, the "red" surface region was not detectable.

In this paper, we provide new observational constraints on the near-infrared colors of (832) Karin and three other Karin family asteroids, based on the data from our past observations in 2003 conducted with the United Kingdom Infra-Red Telescope (UKIRT). Since our observations were made in November 2003, two months after the Sasaki et al. (2004) ob-

Table 1. Summary of observations.

UT	Object	RA	Dec	r [AU]	Δ [AU]	Phase [deg]	Int. [s]	Filters	Note
04:38	(832) Karin	22h04m	$-10°40'$	2.644	2.435	21.9	50–75	$IZJHK$	1st set
05:11	(832) Karin	22h04m	$-10°40'$	2.644	2.435	21.9	150–450	$IZJHK$	2nd set
08:14	(69880) 1998 SQ81	00h41m	$+02°06'$	2.718	1.958	15.7	300–450	IZH	
10:26	(13765) Nansmith	02h19m	$+15°13'$	2.690	1.746	7.6	300–600	IZH	
12:47	(47640) 2000 CA30	04h05m	$+17°16'$	2.714	1.730	2.0	300–450	IZH	
14:35	(4507) Petercollins	09h11m	$+19°14'$	2.840	2.430	19.7	150–600	$IZJHK$	

Note. r and Δ denote the heliocentric and geocentric distances (AU), respectively; Phase is the solar phase angle (deg), and Int. is the total integration time (s).

servations, they may provide valuable insight into the location of the "red" area on the surface of (832) Karin. Additionally, we report the findings regarding (4507) Petercollins, which was initially thought to be a member of the Karin family but was later found not to be.

2. Observations and analysis

Multiband near-infrared images (I, Z, J, H, K bands) of four asteroids in the Karin family—(832) Karin, (13765) Nansmith, (47640) 2000 CA30, and (69880) 1998 SQ81—along with one interloper, (4507) Petercollins, were obtained with the United Kingdom Infrared Telescope (UKIRT) on November 21, 2003. The $IZJHK$ band filters mounted on the UKIRT Fast Track Imager (UFTI) were used for these observations. The I and Z bands correspond to the original UFTI system, while the J, H, and K bands correspond to the Mauna Kea Observatory Near-IR (MKO-NIR) Photometric System (Simons & Tokunaga 2002; Tokunaga & Simons 2002). The I band filter was employed to monitor the magnitude variations due to the asteroid's rotation. For (832) Karin and (4507) Petercollins, the observation filter sequence was $I-Z-I-J-I-H-I-K-I$. Due to limited observation time (only one night), the filter sequence for the other asteroids was restricted to $I-Z-I-H-I$. Integrations were performed using a 5-point jitter pattern. A summary of the observations and ephemerides is presented in table 1.

Photometric calibration was carried out using the UKIRT Faint Standards. Air mass corrections for each band were applied using extinction coefficients obtained from standard star observations. The data were reduced following standard procedures: for each image, bias and dark were subtracted, and then divided by the corresponding flat field. Sky background was also subtracted from each image. The flat fields were created by combining median-filtered night sky frames. These tasks were completed using the IRAF package.

We estimated the solar colors in the near-infrared using the average values of the FS16 (G2) and FS132 (G1) stars from the UKIRT Faint Standards. The average color values were $I-J = 0.31 \pm 0.06$, $I-H = 0.56 \pm 0.07$, and $I-K = 0.72 \pm 0.06$. We adopted $I-Z = 0.15 \pm 0.05$ from FS132, since FS16 does not have a Z-band magnitude.

3. Results

3.1. (832) Karin

The obtained lightcurve of (832) Karin is shown in figure 1. The amplitude of the I-band lightcurve was approximately 0.1 mag. In comparison to the amplitude of 0.61 $\pm$ 0.02 mag for the R-band lightcurve during one rotation in 2003 by Yoshida et al. (2004), the variation of (832) Karin observed in this study is smaller.

A spectrophotometric plot of (832) Karin is shown in figure 2. Since we obtained two data sets, each set is plotted separately. The spectra of the S(IV)-type asteroid (584) Semiramis from the SBN 52 Color Catalog[1] and the L6 ordinary chondrite Paranaiba from the RELAB Public Spectroscopy Database[2] are also shown in figure 2. All the spectra were normalized at 0.952 μm, the bandpass center of the Z-band UFTI filter.

Both spectrophotometric data sets exhibit non-red spectra that are similar to the L6 ordinary chondrite and clearly distinct from the red S(IV)-type spectrum. Similar non-red near-infrared surfaces have also been reported by Chapman et al. (2007) and Vernazza et al. (2007).

3.2. Other Karin family asteroids and (4507) Petercollins

The spectrophotometric results for the Karin family asteroids (13765) Nansmith, (47640) 2000 CA30, and (69880) 1998 SQ81 are shown in figure 3. For (13765) Nansmith and (69880) 1998 SQ81, we obtained only one dataset with I, Z, and H-bands. The spectra of these objects are nearly identical to that of (832) Karin, and are consistent with previous observations made by Vernazza et al. (2006). Our observations provide a single snapshot of each asteroid. However, the fact that our observations and those by Vernazza et al. (2006) (conducted on different dates) yielded almost identical spectra suggests that these asteroids have uniform surface colors.

For (47640) 2000 CA30, the Z- and H-band spectra exhibit trends similar to those of (13765) Nansmith and (69880) 1998 SQ81, whereas the I-band spectrum shows a significantly lower reflectance.

(4507) Petercollins was initially classified as the second-largest member of the Karin family (Nesvorný et al. 2002), but

[1] https://pds-smallbodies.astro.umd.edu/
[2] https://sites.brown.edu/relab/relab-spectral-database/

was later regarded as an interloper and excluded from the family in a subsequent study (Nesvorný & Bottke 2004). The visible spectrum of (4507) Petercollins was reported to be much redder than that of (832) Karin, with a shallower absorption feature near 1 micron (Vernazza et al. 2006). We confirm that (4507) Petercollins is also redder in the near-infrared. In fact, the spectrum of (4507) Petercollins was significantly redder than those of the other Karin family asteroids in our observations.

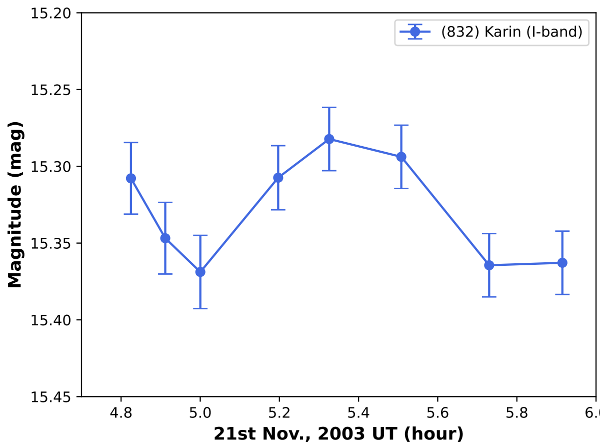

Fig. 1. Lightcurve of (832) Karin in the I-band.

4. Discussion

We attempt to estimate the location of the "red" area on (832) Karin based on both our observations and previous data. Our observations of (832) Karin were conducted on November 21, 2003, approximately two months after those by Yoshida et al. (2004) and Sasaki et al. (2004). The synodic rotation period of (832) Karin has been determined to be 18.35 $\pm$ 0.02 hr (Yoshida et al. 2004). We calculated the rotation phase (ϕ) at the time of our observations to constrain the location of the "red" area relative to the rotation phase. We took into account the uncertainty in the rotation period ($\pm$0.02) and obtained the rotational phases ϕ = 0.87$\pm$0.10 to 0.00$\pm$0.12, corresponding to the lightcurve maximum, during which the red region was not in view. We did not consider changes in the apparent viewing geometry of (832) Karin in the calculations, as the differences in ecliptic coordinates between the observations were small. From September to November 2003, (832) Karin remained nearly stationary in the sky, although its distance from Earth (Δ) did change.

Combining the observations by Yoshida et al. (2004) and Sasaki et al. (2004), the "red" area was observed around the lightcurve minimum, at rotation phases ϕ = 0.20 to 0.33. A drastic change from "red" to "non-red" was observed beyond ϕ = 0.34, marking the boundary between the first and second sets of observations by Sasaki et al. (2004). The rotation phase at each observation is shown in table 2.

Next, we examined the viewing geometry of (832) Karin during the 2003, 2004, and 2006 observations. The "red" area

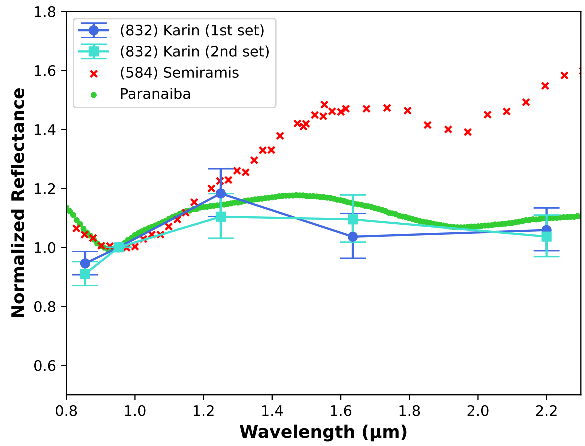

Fig. 2. Spectrophotometric results of (832) Karin normalized at 0.952 μm. The spectra of the S(IV)-type asteroid (584) Semiramis and the L6 ordinary chondrite Paranaiba are also shown for comparison.

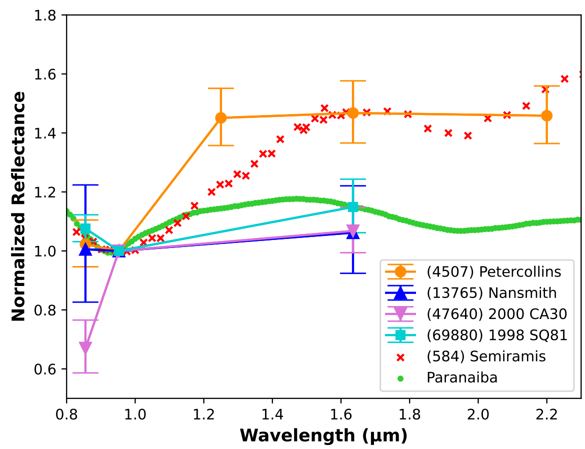

Fig. 3. Spectrophotometric results of Karin family asteroids (13765) Nansmith, (47640) 2000 CA30, (69880) 1998 SQ81, and the interloper (4507) Petercollins. The spectra of the S(IV)-type asteroid (584) Semiramis and the L6 ordinary chondrite Paranaiba are also shown for comparison.

was observed in 2003, but was not observed in 2004 and 2006. We attempted to use these observations to place further constraints on the location of the "red" area.

To date, the DAMIT database[3] (Ďurech, Sidorin, & Kaasalainen 2010) provides the two possible shape and pole solutions for (832) Karin: (λ_1, β_1) = (59°,44°) and (λ_2, β_2) = (242°,46°) (Hanuš et al. 2011). Using these solutions, we calculated the aspect angles ψ_1 and ψ_2 for each previous observation, where each angle is defined as the angle between the pole and the object–observer line (see table 3). We focused on the pole solution (λ_1, β_1) = (59°,44°), since ψ_1 and ψ_2 are symmetric with respect to the equatorial plane of (832) Karin.

Our results indicate that the 2003 observation was made from the equatorial direction, while the 2004 and 2006 observa-

[3] https://astro.troja.mff.cuni.cz/projects/damit/

tions were made from the southern and northern hemispheres, respectively (see figure 4).

Since the 2004 southern observations by Ito & Yoshida (2007) did not detect the “red” area over a full rotation, we infer that this area may be located in the northern hemisphere, which was not visible during their observations. However, Chapman et al. (2007) and Vernazza et al. (2007) reported that no “red” spectrum was observed throughout the rotation phase in the 2006 northern observations. These results suggest that the “red” area is visible only from equatorial views; i.e., it is not detectable from oblique viewing angles. This provides another constraint on the location of the “red” area of (832) Karin.

If Karin’s surface truly exhibited a persistent red-colored area, it should have reappeared in at least one of the later observations. However, the red area was not seen, implying that it would have to lie in a highly specific topography—for example, inside a crater or a steep depression, possibly near the equator, that becomes visible only within a narrow range of illumination and viewing aspect. In such a case, the feature would appear only momentarily and disappear with even a slight change in geometry.

This scenario also requires a strong spectral contrast relative to the surrounding terrain. While we cannot fully rule out such a small, topographically confined region, we consider the existence of a stable, distinct “red” area on (832) Karin unlikely.

Table 2. Rotational phase and color of (832) Karin during the 2003 observations.

Phase	Red or not	Note
0.87±0.10	non-red	this work (1st set)
0.00±0.12	non-red	this work (2nd set)
0.20–0.24	red	Yoshida et al. (2004)
0.30–0.34	red	Sasaki et al. (2004) (1st set)
0.35–0.38	non-red	Sasaki et al. (2004) (2nd set)
0.45–0.50	non-red	Sasaki et al. (2004) (3rd set)

Note. The uncertainties in the rotational phase for the first and second data sets arise from the uncertainty in the rotation period (± 0.02 hr).

Acknowledgments

We thank the anonymous referee for constructive comments that improved the manuscript. This research was supported by MEXT as “Developing a Research Data Ecosystem for the Promotion of Data-Driven Science,” and by JSPS KAKENHI (21H01142, 21H05420, 23K20872). We used “mdx: a platform for building data-empowered society” for the data analysis (Suzumura et al. 2022).

References

Chapman, C. R., Enke, B., Merline, W. J., Tamblyn, P., Nesvorný, D., Young, E. F., & Olkin, C. 2007, Icarus, 191, 323

Davis, D. R., Weidenschilling, S. J., Farinella, P., Paolicchi, P., & Binzel, R. P. 1989, in Asteroids II, ed. R. P. Binzel, T. Gehrels, & M. S. Matthews (Tucson: University of Arizona Press), 805

Ďurech, J., Sidorin, V., & Kaasalainen, M. 2010, A&A, 513, A46

Hanuš, J., et al. 2011, A&A, 530, A134

Harris, A., Mueller, M., Lisse, C., & Cheng, A. 2009, Icarus, 199, 86

Ito, T., & Yoshida, F. 2007, PASJ, 59, 269

Nesvorný, D., & Bottke, W. F. 2004, Icarus, 170, 324

Nesvorný, D., Bottke, W. F., Jr., Dones, L., & Levison, H. F. 2002, Nature, 417, 720

Sasaki, T., et al. 2004, ApJ, 615, L161

Simons, D. A., & Tokunaga, A. 2002, PASP, 114, 169

Suzumura, T., et al. 2022, in Proc. 2022 IEEE Intl Conf on Dependable, Autonomic and Secure Computing, Intl Conf on Pervasive Intelligence and Computing, Intl Conf on Cloud and Big Data Computing, Intl Conf on Cyber Science and Technology Congress (DASC/PiCom/CBDCom/CyberSciTech), 1

Tokunaga, A. T., & Simons, D. A. 2002, PASP, 114, 180

Vernazza, P., Rossi, A., Birlan, M., Fulchignoni, M., Nedelcu, D. A., & Dotto, E. 2007, Icarus, 191, 330

Vernazza, P., et al. 2006, A&A, 460, 945

Yoshida, F., et al. 2004, PASJ, 56, 1105

Yoshida, F., et al. 2016, Icarus, 269, 15

Zappalà, V., Farinella, P., Knežević, Z., & Paolicchi, P. 1984, Icarus, 59, 261

Table 3. Position (λ, β), distance (r, Δ), and aspect angles ψ_1, ψ_2 for each observation.

Obs. No.	Date	λ (deg)	β (deg)	r (AU)	Δ (AU)	ψ_1 (deg)	ψ_2 (deg)	Reference
1	4 Sep. 2003	328.2	1.6	2.677	1.685	90	94	Yoshida et al. (2004)
2	14 Sep. 2003	326.4	1.5	2.672	1.724	89	95	Sasaki et al. (2004)
3	21 Nov. 2003	329.4	1.1	2.644	2.433	91	93	this work
4	22 Apr. 2004	80.8	0.3	2.693	2.696	136	46	Ito & Yoshida (2007)
5	7 Jan. 2006	176.0	-1.2	3.049	2.562	70	106	Chapman et al. (2007)
6	29 Jan. 2006	176.0	-1.3	3.059	2.302	70	105	Vernazza et al. (2007)
7	17 Apr. 2006	163.0	-1.3	3.085	2.281	79	97	Vernazza et al. (2007)

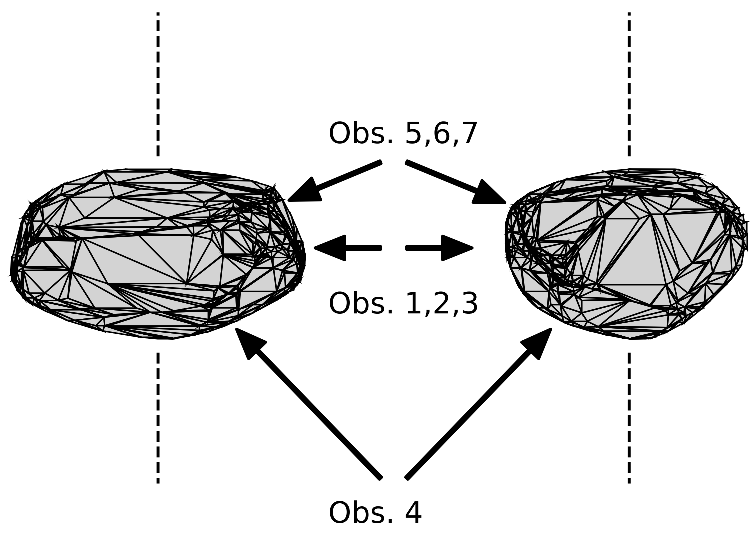

Fig. 4. Schematic views of (832) Karin observations. Each arrow indicates the direction from the observer to (832) Karin. The direction was calculated using the pole solution $(\lambda, \beta) = (59°, 44°)$. The dashed line represents the rotation axis. Observation numbers correspond to those listed in table 3. The past observations were conducted from various aspect angles, including northern, equatorial, and southern views. The "red" area was observed only at observation numbers 1 and 2.